Appl. Math. Mech. -Engl. Ed., **38**(11), 1565–1578 (2017)
DOI 10.1007/s10483-017-2273-9

Applied Mathematics and Mechanics (English Edition)

Comprehensive investigation of stress intensity factors in rotating disks containing three-dimensional semi-elliptical cracks*

M. FAKOOR†, S. M. N. GHOREISHI

Faculty of New Sciences and Technologies, University of Tehran, Tehran 14395-1561, Iran

Abstract Initiation and propagation of cracks in rotating disks may cause catastrophic failures. Therefore, determination of fracture parameters under different working conditions is an essential issue. In this paper, a comprehensive study of stress intensity factors (SIFs) in rotating disks containing three-dimensional (3D) semi-elliptical cracks subjected to different working conditions is carried out. The effects of mechanical properties, rotational velocity, and orientation of cracks on SIFs in rotating disks under centrifugal loading are investigated. Also, the effects of using composite patches to reduce SIFs in rotating disks are studied. The effects of patching design variables such as mechanical properties, thickness, and ply angle are investigated separately. The modeling and analytical procedure are verified in comparison with previously reported results in the literature.

Key words stress intensity factor (SIF), semi-elliptical crack, rotating disk, finite element analysis (FEA)

Chinese Library Classification O346.1
2010 Mathematics Subject Classification 74R10

1 Introduction

Rotating disks are employed in various industrial applications such as aerospace and automotive industries. Initiation and propagation of cracks in rotating disks may cause catastrophic failures. Thus, to assure the safety of rotating disks in service, an accurate fracture mechanics analysis instead of the conventional design method is required. Stress intensity factors (SIFs) are the basic parameters for investigation of fracture behavior in cracked rotating disks. These parameters play an important role in linear elastic fracture mechanics (LEFM). Available methods for extraction of SIFs include singular integral equations[1–3], weight functions[4–7], boundary collocation[8–9], finite element[10–13], boundary element[14–15], extended finite element method (FEM), and combination methods[16–18]. Calculation of the SIFs in a finite elastic domain with numerical solution of singular integral equations may be a popular approach. The weight function method is an alternative simple technique for calculation of SIFs in a finite elastic domain when suitable weight functions are available. Also, the boundary collocation method is another suitable way for extraction of SIFs. However, the FEM is known as an adaptable and efficient approach. In this method, singular elements near the crack tip are required. The boundary element method requires only the discretization of the boundary. The boundary element method

* Received Dec. 1, 2016 / Revised May 7, 2017
† Corresponding author, E-mail: mfakoor@ut.ac.ir

is simple to be employed, but the results are not as accurate as those of the FEM. Moreover, some mixed and combination methods are utilized to calculate the SIFs.

Due to importance of fracture behavior investigation in rotating disks, several studies have been carried out to evaluate the crack tip parameters. Mechanical strength, life estimation, and calculation of SIFs are issues which are paid much attention to in the recent studies in the field of rotating cracked disks. Rooke and Tweed[19] derived the Fredholm integral equation for a rotating disk containing radial crack. They defined the SIFs for symmetrical loading types numerically, using the Gauss-Chebyshev quadrature formula. Blauel et al.[20] solved the same problem by utilizing a photo-elastic method and a simple super-position procedure. Employing a rough finite element procedure, Chan et al.[21] determined the approximated SIFs for rotating fracture test specimens. Gowhari-Anaraki et al.[22] estimated the C^*-integral for radial cracks in annular discs. Constant angular velocity and internal pressure were considered in their study. Lorenzo and Cartwright[23] studied the boundary element weight function for an internal edge crack in a rotating annular disk. Since the weight function can eliminate the body force term in the boundary element formulation, this effect was reduced to boundary traction by utilizing Bueckner's principle. A rotating compound disk containing a radial crack was studied, and the SIFs of the crack were calculated by Xu[24]. He presented extensive numerical results for both plane strain and plane stress cases in tabular and graphical forms. Bowie and Neal[25] and Isida[26] also utilized numerical methods for calculation of SIFs of cracked disks. Despite other studies that used two-dimensional (2D) models, Pook et al.[27] used a three-dimensional (3D) finite element model for investigation of fracture parameters in a cracked disk under anti-plane loading. They showed that utilizing 3D models for investigation of fracture parameters in rotating disks can lead to more accurate results than 2D models. Kotousov et al.[10] also used 3D models for calculation of the SIFs.

Regarding the above literature, it is found that until now, few studies have used 3D models for calculation of the fracture parameters in rotating disks. Also, the effects of different parameters such as mechanical properties, rotational velocity, and orientation of cracks have not been considered. Moreover, comprehensive studies on the effects of employing composite patches in the SIFs for cracked rotating disks are not found in the literature. Therefore, in this research, an extensive study is performed for calculation of SIFs in rotating disks containing 3D semi-elliptical cracks. Also, various conditions are considered for mechanical properties, rotational velocity, and crack orientation. The effects of utilizing composite patches in reduction of SIFs are studied. Moreover, effective design variables such as mechanical properties, thickness, and ply angle are investigated for composite patches, separately.

2 3D finite element modeling of semi-elliptical cracks

Lin and Smith[28] showed that any kind of crack changes to semi-elliptical cracks after propagation. Therefore, the surface cracks can be assumed as semi-elliptical cracks. Thus, in this section, 3D semi-elliptical cracks in rotating disks are modeled in the ABAQUS software. In this regard, several circumferential and radial semi-elliptical cracks with the aspect ratio of a/c 0.4 to 1 are modeled in the ABAQUS software. All modeled cracks have fixed length of 10 mm, and their aspect ratio takes the depth of 2 mm to 5 mm.

Figure 1 shows radial and circumferential semi-elliptical cracks in a rotating disk, schematically. The geometrical dimensions and material properties which are used in a finite element analysis (FEA) are listed in Table 1.

The created 3D models of rotating disk with different crack depths are meshed utilizing a total number of 40 635 solid C3D20 elements in the ABAQUS software. Typical 3D mesh pattern generated for the mentioned rotating disk and a zoomed view of the crack tip region are shown in Fig. 2. To include crack tip singularity in the created model, a special element, which is called the singular element, is considered. This is performed by moving

the first ring mid-side nodes around the crack front to the quarter distance near the crack front nodes.

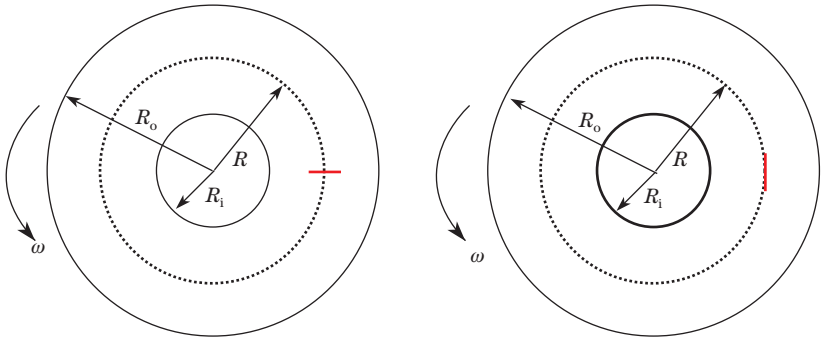

Fig. 1 Radial semi-elliptical crack (Case 1) and circumferential semi-elliptical crack (Case 2) in rotating disk, schematically

Table 1 Geometrical dimensions and material properties which are used in FEA

Parameter	Definition	Value
R_i	Inner radius of rotating disk	10 cm
R_o	Outer radius of rotating disk	30 cm
R	Position of semi-elliptical cracks	20 cm
t	Thickness of rotating disk	2 cm
$2c$	Length of semi-elliptical cracks	5 mm
a	Depth of semi-elliptical cracks	From 2 mm to 5 mm
E_{St}	Elastic modulus of steel	200 GPa
E_{Al}	Elastic modulus of aluminum	71 GPa
υ_{St}	Poisson's ratio of steel	0.30
υ_{Al}	Poisson's ratio of aluminum	0.33
ρ_{St}	Steel density	7 850 kg/m^3
ρ_{Al}	Aluminum density	2 770 kg/m^3

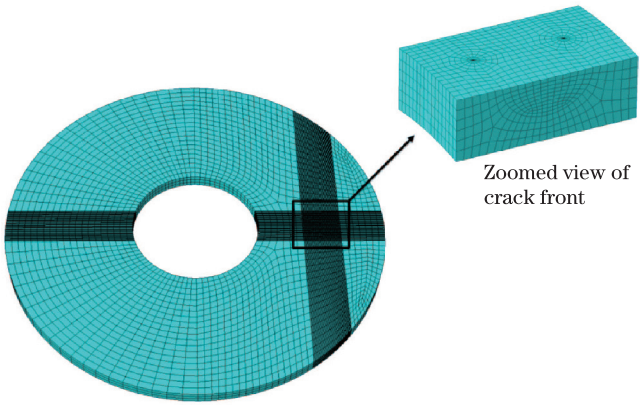

Fig. 2 3D mesh pattern generated for rotating disk and zoomed view of crack tip region

Geometry of semi-elliptical cracks in the rotating disks can be identified with the disk thickness (t), inside and outside radii of the disk (i.e., R_i and R_o), the crack length (c), and the crack

depth (a). Semi-elliptical cracks are modeled by the length of crack along the major axis of ellipse and the depth of crack in accordance with the minor ellipse axis. Figure 3 represents the crack face and the points on the crack face on which the SIFs are derived. For simplification in determination of the points on the crack face, at first, the x-coordinate is defined and then points on the crack face prescribed by a dimensionless distance of x/c. As shown in Fig. 3, the origin of x-coordinate is located at the free surface of crack front.

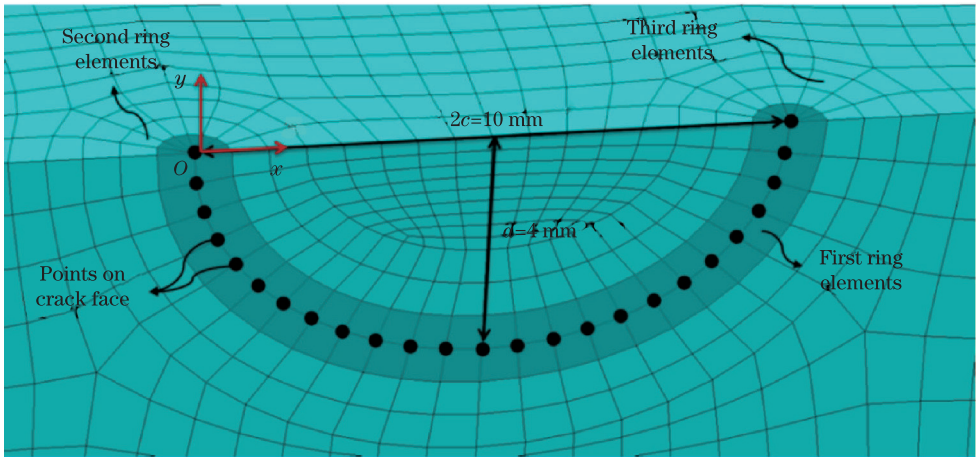

Fig. 3 Crack face and points on crack face for semi-elliptical crack with aspect ratio 0.8

A 3D finite element model should have an optimal number of elements to perform an accurate numerical analysis. For determination of the optimal number of elements to ensure the accuracy of results, the convergence analysis should be performed. In this regard, the maximum value of the mode I SIF for radial semi-elliptical cracks in the rotating disk with different aspect ratios (a/c) and different numbers of elements are calculated. Results of convergence analysis for determination of a sufficient number of elements are shown in Fig. 4. According to this figure, it is revealed that, after about 40 000 elements, the finite element results are converged.

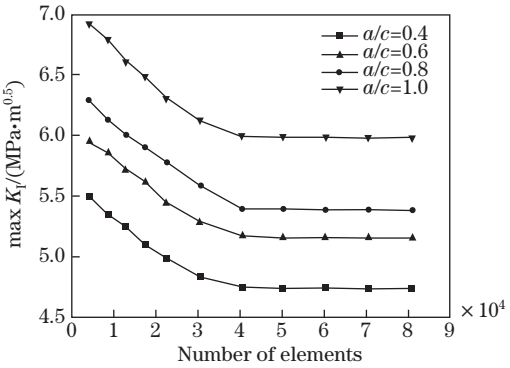

Fig. 4 Convergence of maximum mode I SIF for radial semi-elliptical cracks in rotating disk

Therefore, the optimum number of elements in the numerical modeling is approximately around 40 000 elements.

3 Calculation of SIFs

In the LEFM, the stress state near the crack tip under a general mixed mode loading can be written from William's solution[29],

$$\sigma_r = \frac{1}{4\sqrt{2\pi r}}\Big(K_{\mathrm{I}}\Big(5\cos\frac{\theta}{2} - \cos\frac{3\theta}{2}\Big) + K_{\mathrm{II}}\Big(-5\sin\frac{\theta}{2} + 3\sin\frac{3\theta}{2}\Big)\Big) + T\cos^2\theta + O(r^{1/2}), \tag{1}$$

$$\sigma_\theta = \frac{1}{4\sqrt{2\pi r}}\Big(K_{\mathrm{I}}\Big(3\cos\frac{\theta}{2} + \cos\frac{3\theta}{2}\Big) - K_{\mathrm{II}}\Big(3\sin\frac{\theta}{2} + 3\sin\frac{3\theta}{2}\Big)\Big) + T\sin^2\theta + O(r^{1/2}), \tag{2}$$

$$\sigma_z = \begin{cases} 0 \quad \text{(plane stress)}, \\ \dfrac{8\upsilon}{4\sqrt{2\pi r}}\Big(K_{\mathrm{I}}\cos\dfrac{\theta}{2} - K_{\mathrm{II}}\sin\dfrac{\theta}{2}\Big) + T + O(r^{1/2}), \end{cases} \tag{3}$$

$$\sigma_{r\theta} = \frac{1}{4\sqrt{2\pi r}}\Big(K_{\mathrm{I}}\Big(\sin\frac{\theta}{2} + \sin\frac{3\theta}{2}\Big) + K_{\mathrm{II}}\Big(\cos\frac{\theta}{2} + 3\cos\frac{3\theta}{2}\Big)\Big) - T\sin\theta\cos\theta + O(r^{1/2}), \tag{4}$$

$$\sigma_{z\theta} = \frac{1}{\sqrt{2\pi r}}K_{\mathrm{III}}\cos\frac{\theta}{2} + O(r^{1/2}), \tag{5}$$

$$\sigma_{rz} = \frac{1}{\sqrt{2\pi r}}K_{\mathrm{III}}\sin\frac{\theta}{2} + O(r^{1/2}), \tag{6}$$

where r and θ are the conventional crack tip coordinates which are defined in Fig. 5. K_{I}, K_{II}, and K_{III} are the SIFs in the modes I, II, and III, respectively. These factors are the most important parameters in the LEFM.

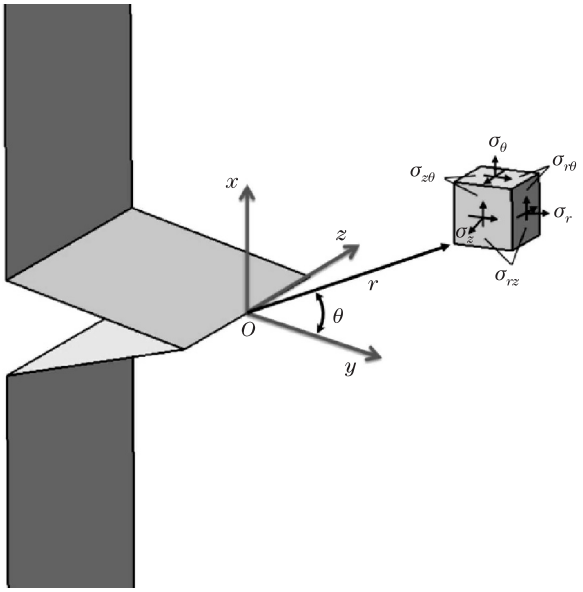

Fig. 5 Definition of conventional crack tip coordinate

In the rotating disks, these factors are functions of load, crack length, crack depth, and geometry. These coefficients can be expressed as[30]

$$\begin{cases} K_{\mathrm{I}} = Y_{\mathrm{I}}\Big(\dfrac{a}{c}, \dfrac{a}{t}, \dfrac{R_{\mathrm{i}}}{R_{\mathrm{o}}}\Big)\sigma_0\sqrt{\pi a}, \\ K_{\mathrm{II}} = Y_{\mathrm{II}}\Big(\dfrac{a}{c}, \dfrac{a}{t}, \dfrac{R_{\mathrm{i}}}{R_{\mathrm{o}}}\Big)\sigma_0\sqrt{\pi a}, \\ K_{\mathrm{III}} = Y_{\mathrm{III}}\Big(\dfrac{a}{c}, \dfrac{a}{t}, \dfrac{R_{\mathrm{i}}}{R_{\mathrm{o}}}\Big)\sigma_0\sqrt{\pi a}, \end{cases} \tag{7}$$

in which Y_{I}, Y_{II}, and Y_{III} are geometrical coefficients in the modes I, II, and III, respectively. σ_0 is the nominal stress, and in the rotating disks, it can be expressed as

$$\sigma_0 = \frac{3+\upsilon}{8}\rho\omega^2(R_{\mathrm{o}}^2 - R_{\mathrm{i}}^2). \tag{8}$$

Rotating disks are commonly encountered to the emergence of the only mode I SIF (i.e., SIFs in the modes II and III are negligible). In particular cases, whenever the geometry condition and loading are not elaborate, the SIFs can be evaluated by analytical methods. However, in most practical cases where the problem is more complicated (such as 3D cracks in rotating disks), numerical methods (such as the FEM) should be employed. In the FEM, some methods such as virtual crack growth[31] and J integral[32] are available for computing the SIFs. The J integral on the crack tip Γ contour is defined as[33]

$$J = \int_{\Gamma}\Big(W\mathrm{d}y - T_i\frac{\partial u_i}{\partial x}\mathrm{d}s\Big), \tag{9}$$

where T and u are the traction and displacement vectors, respectively. Also, Γ is a closed contour, and $\mathrm{d}s$ is the element of the arc along the path Γ. By considering Γ as a counterclockwise path, we have

$$\mathrm{d}x = -n_y\mathrm{d}s, \quad \mathrm{d}y = n_x\mathrm{d}s, \quad T_i = n_j\sigma_{ij}, \tag{10}$$

where n_x, n_y, and n_j are direction cosines. By substituting Eq. (10) into Eq. (9), we have

$$J = \int_{\Gamma}\Big(Wn_x - n_j\sigma_{ij}\frac{\partial u_i}{\partial x}\Big)\mathrm{d}s. \tag{11}$$

From Green's theorem, we have

$$\int_{\Gamma} f_j n_j \mathrm{d}\Gamma = \int_A \frac{\partial f_j}{\partial x_j}\mathrm{d}A. \tag{12}$$

By using this result, we can express Eq. (11) as follows:

$$J = \int_A \frac{\partial}{\partial x_j}\Big(W\delta_{1j} - \sigma_{ij}\frac{\partial u_i}{\partial x}\Big)\mathrm{d}A, \tag{13}$$

where A is the surface between two contours (including the crack). Also, W in Eq. (13) represents the strain energy density and is calculated as

$$W = \int \sigma_{ij}\mathrm{d}\varepsilon_{ij} = \frac{1}{2}\sigma_{ij}\varepsilon_{ij}. \tag{14}$$

In this paper, a J integral based method built in the ABAQUS software is employed for obtaining SIFs directly from a static analysis of rotating disks. The obtained results from the FEA for different working conditions in the rotating disks are presented and discussed in the following sections.

4 Numerical results of SIFs in rotating disks

Variations of the mode I SIFs through the crack front for radial and circumferential semi-elliptical cracks in the steel and aluminum rotating disks are illustrated in Figs. 6 and 7, respectively. The aspect ratio is considered from 0.4 to 1, and the rotational velocity is 6 000 r/min. According to these figures, it is revealed that, regardless of mechanical properties of rotating disks and orientation of cracks, the maximum value of K_{I} in the aspect ratios of 0.4 and 0.6 is achieved in the deepest point of crack front. Also, the maximum value of K_{I} in the aspect ratios of 0.8 and 1 is achieved in the free surfaces of crack front. Thus, propagation of cracks in the rotating disks initiates from the deepest point and free surfaces of crack front for the cracks with aspect ratios of 0.4 to 0.6 and aspect ratios of 0.8 to 1, respectively.

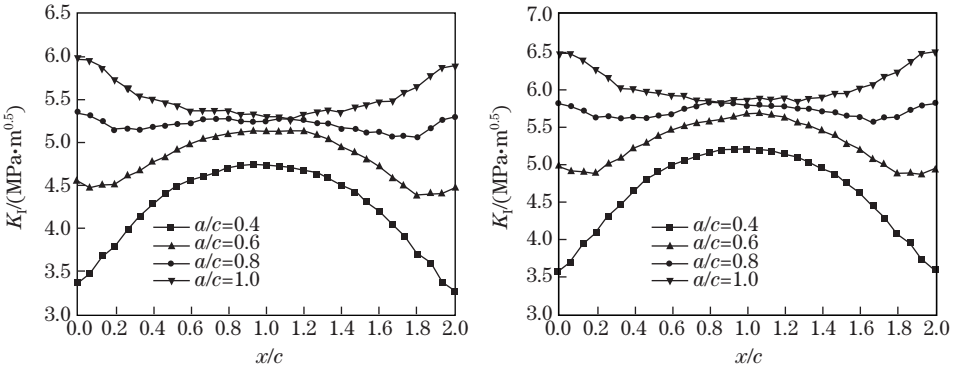

(a) Radial semi-elliptical crack (b) Circumferential semi-elliptical crack

Fig. 6 Variations of mode I SIF through crack front in steel rotating disk with rotational velocity of 6 000 r/min and different aspect ratios

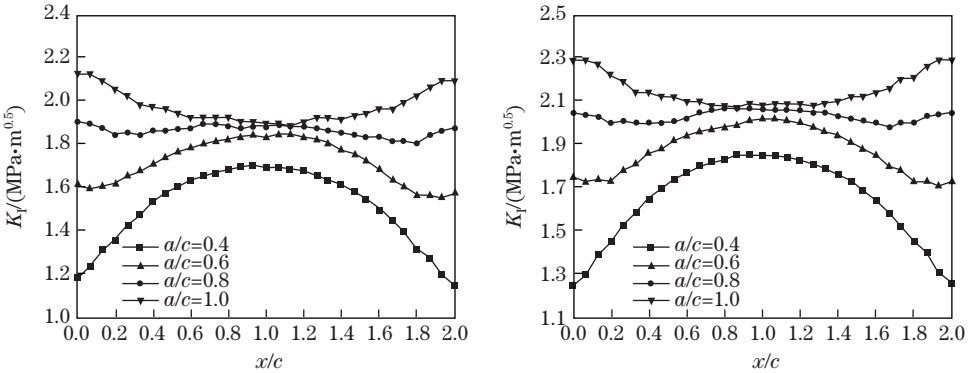

(a) Radial semi-elliptical crack (b) Circumferential semi-elliptical crack

Fig. 7 Variations of mode I SIF through crack front in aluminum rotating disk with rotational velocity of 6 000 r/min and different aspect ratios

The results of the mode I SIF for radial and circumferential semi-elliptical cracks of steel and aluminum rotating disks are compared with each other in Fig. 8. The aspect ratio is 0.8, and the rotational velocity is assumed to be 6 000 r/min. According to this figure, the values of the SIFs for circumferential cracks are larger than those for radial cracks in both steel and aluminum rotating disks. Thus, regardless of mechanical properties of rotating disks, circumferential cracks are identified as crucial cracks in rotating disks.

To investigate the effects of the rotational velocity on SIFs, variations of K_{I} through the crack front for circumferential semi-elliptical cracks with the aspect ratio of 0.8 in the steel

and aluminum rotating disks with the rotational velocity of 6 000 r/min to 9 000 r/min are illustrated in Fig. 9. According to this figure, it is shown that the values of the SIFs (for both steel and aluminum rotating disks) increase via increasing the rotational velocity of rotating disks. Also, from this figure, it is found that by increasing the rotational velocity from 6 000 r/min to 9 000 r/min, the maximum increase in the mode I SIFs are 102 and 112 percent for steel and aluminum rotating disks, respectively. Thus, aluminum rotating disks have higher sensitivity to the increase of rotational velocity than the steel rotating disks.

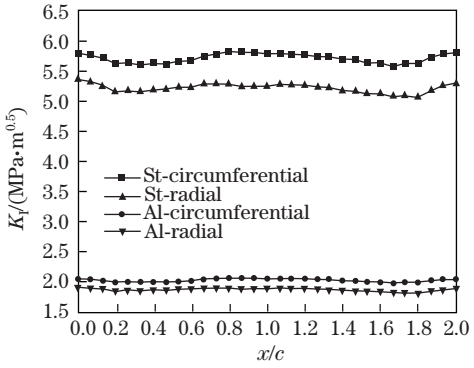

Fig. 8 Comparison of K_I through crack front for radial and circumferential semi-elliptical cracks with aspect ratio of 0.8 in steel and aluminum rotating disks with rotational velocity of 6 000 r/min

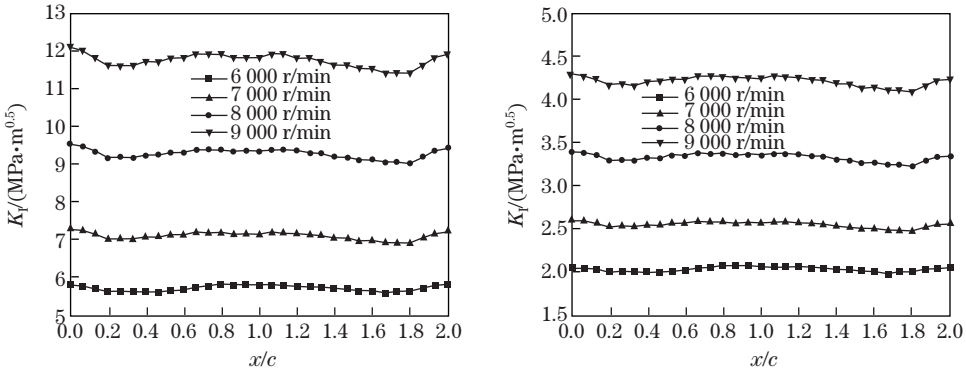

Fig. 9 Variations of mode I SIF through crack front for circumferential semi-elliptical cracks with aspect ratio of 0.8 and different rotational velocities for steel and aluminum rotating disks

5 Numerical results of SIFs in rotating disks containing composite patch

A repair method utilizing a composite patch to reinforce the cracked structures has been known as an effective approach due to the light weight and high strength of composite materials[34–37]. This repairing method was initially investigated in Australia in the early 1970s and later in USA in the 1980s[38]. Numerous models have been developed for analysis of repairs utilizing various calculation techniques including the collocation method, the boundary element method, and the FEM[39–42]. Due to well established role of SIF in fracture mechanics, the SIF is an important measure for analyzing the performance of composite patch in repairing cracks.

The aim of this section is to investigate the effects of composite reinforcement on the fracture resistance of cracked rotating disks under a centrifugal loading. For this purpose, several 3D semi-elliptical cracks are modeled without and with the use of composite patch in the rotating disks. Figure 10 shows radial and circumferential semi-elliptical cracks in the rotating disk with a composite patch, schematically. The fiber composites carbon/epoxy and glass/epoxy have been frequently used in the literature for patching or reinforcing the cracked structures. Therefore, to investigate the mechanical properties effectively, both the composite patches are considered for finite element modeling. The composite patch is bonded on one side of the disk, using a thin layer of adhesive. The shear modules and the thickness of adhesive film are assumed to be 350 MPa and 0.05 mm, respectively. The dimension of the composite patch is 7×7 cm^2, and as shown in Fig. 10, the crack is located in the middle line of the patch. The composite patch is assumed as a unidirectional ply and is modeled using a total number of 2 183 shell S4R elements in the ABAQUS software.

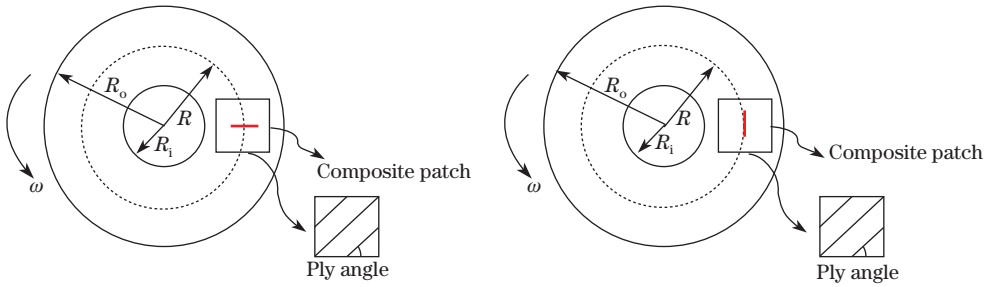

Fig. 10 Radial semi-elliptical crack (Case 3) and circumferential semi-elliptical crack (Case 4) in rotating disk with composite patch, schematically

A 3D model which is provided for the FEA of the cracked disk and the composite patch is shown in Fig. 11.

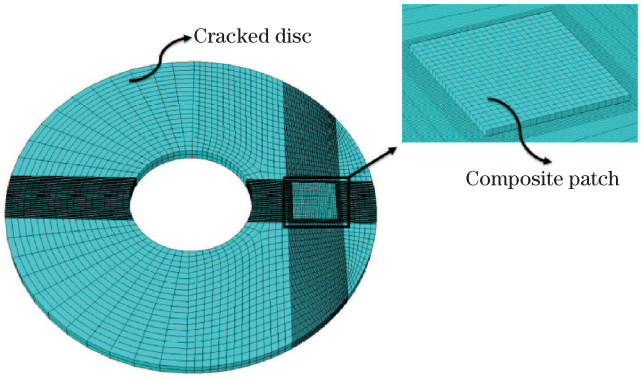

Fig. 11 3D model provided for FEA of cracked disk and composite patch

The material properties for composite patches are given in Table 2.

Table 2 Properties for composite patches

Material	E_1/GPa	E_2/GPa	υ_{12}	G_{12}/GPa	ρ/(kg·m^{-3})
Carbon/epoxy	121	8.6	0.27	4.7	1 490
Glass/epoxy	50	8.0	0.30	5.0	2 000

Figures 12 and 13 show the variations of K_{I} through the crack front for radial and circumferential semi-elliptical cracks with the aspect ratio of 0.8 in the steel rotating disk with the rotational velocity of 9 000 r/min without and with the use of composite patches for the thickness of 0.25 mm and different ply angles, respectively. It is found that the patching reinforcement considerably decreases the SIFs. This effect can be interpreted for various reinforced configurations such as the load carrying capacity of patches in the cracked region. It is found that the carbon/epoxy patch decreases K_{I} more than the glass/epoxy patch. It means that stiffer patch materials are desirable for cracked rotating disks. Also, from these figures, it is found that the SIF values for radial cracks are lower than circumferential cracks. Therefore, using the composite patch in the rotating disks has the maximum effect on radial cracks. Also, the results indicate that, in the rotating disks, regardless of mechanical properties of composite patches and orientation of cracks, the best value for a ply angle is 90°.

To investigate the effects of the composite patch thickness on the SIFs, the variations of K_{I} through the crack front for circumferential semi-elliptical cracks with the aspect ratio 0.8 in the steel rotating disk with the rotational velocity 9 000 r/min and different thicknesses of composite patch are illustrated in Fig. 14. According to this figure, it is found that the SIF values (for both carbon/epoxy and glass/epoxy patches) are diminished via increasing the thickness of the composite patch. Therefore, this method can be considered as an effective solution for reinforcement of the cracked rotating disks in practical situations.

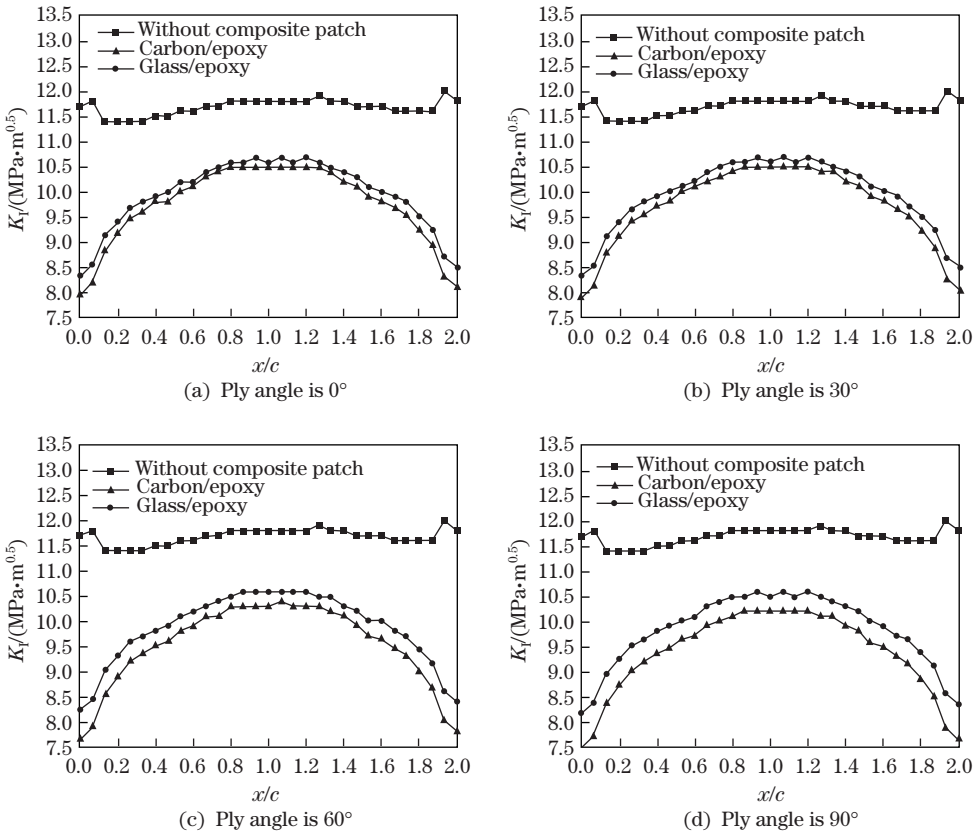

Fig. 12 Variations of mode I SIF through crack front for radial semi-elliptical cracks (Case 3) with aspect ratio 0.8 in steel rotating disk with rotational velocity 9 000 r/min without and with use of composite patches for thickness of 0.25 mm and different ply angles

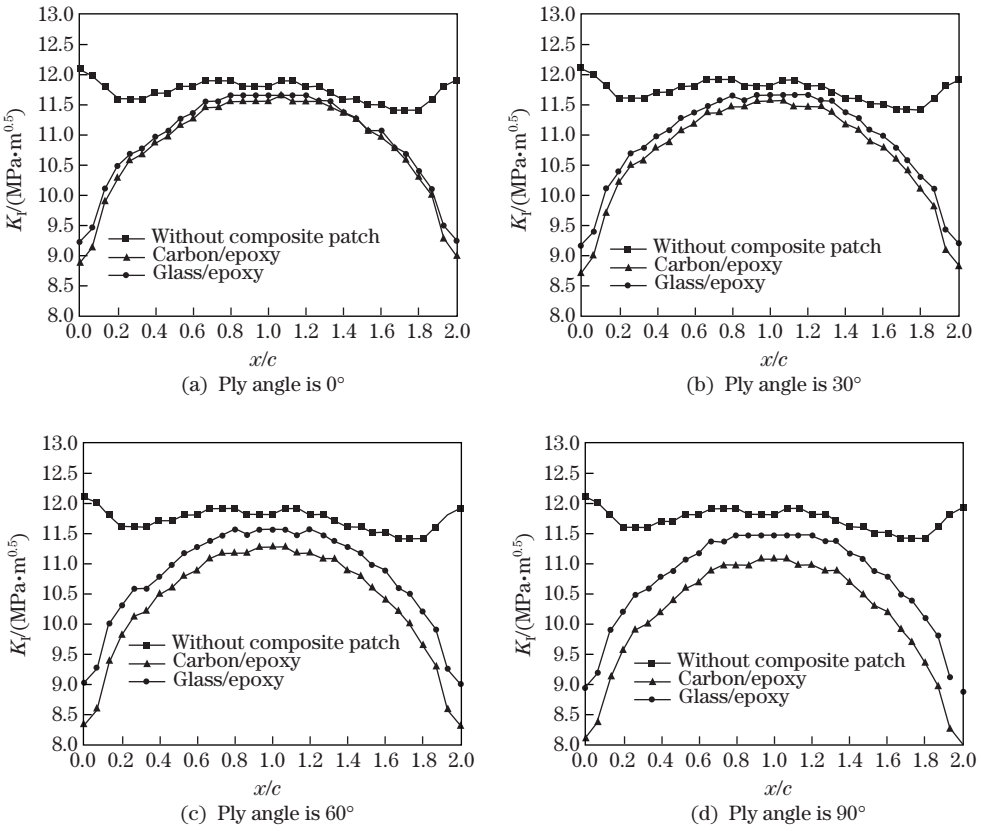

Fig. 13 Variations of mode I SIF through crack front for circumferential semi-elliptical cracks (Case 4) with aspect ratio 0.8 in steel rotating disk with rotational velocity 9 000 r/min without and with use of composite patches for thickness of 0.25 mm and different ply angles

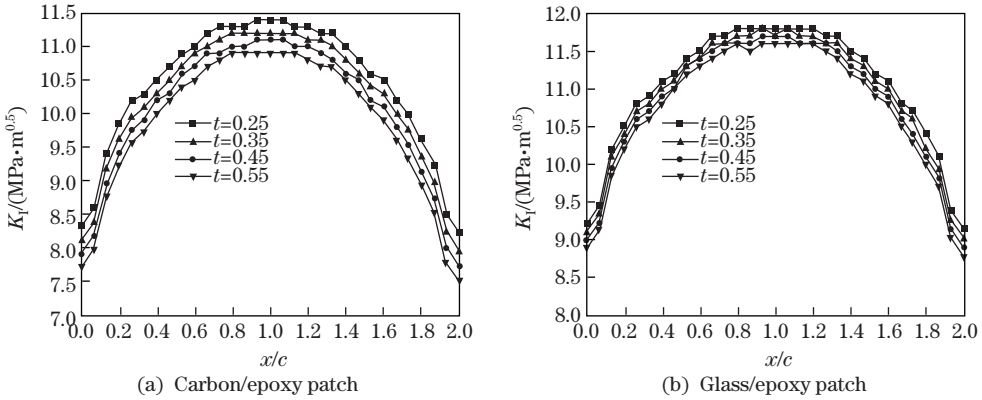

Fig. 14 Variations of mode I SIF through crack front for circumferential semi-elliptical cracks with aspect ratio 0.8 in steel rotating disk with rotational velocity 9 000 r/min and different thicknesses of carbon/epoxy patch and glass/epoxy patch

6 Verification procedure of modeling and analysis

In this section, our modeling and analysis procedure is confirmed by previously well-accepted related studies. In this regard, we consider the research results of Nami and Eskandari[43] which

have been performed for calculation of SIFs in a rotating impeller containing semi-elliptical surface crack. They considered a steel impeller and calculated the SIFs utilizing a 3D finite element model for a circumferential crack in the mentioned rotating impeller. The employed geometrical dimensions and material properties by Nami and Eskandari[43] are listed in Table 3.

Table 3 Employed geometrical dimensions and material properties in Ref. [43]

Parameter	Value
Inside diameter	140 mm
Outside diameter	414 mm
Position of crack (radius)	120 mm
Wall thickness	6 mm
Rotation speed	8 500 r/min
Module of elasticity	210 GPa
Poisson's ratio	0.3
Density	7 850 kg/m^3

In order to ensure from our modeling and analysis procedure, the mentioned rotating impeller is modeled in the ABAQUS software, and the results associated with the SIFs are compared with those reported in Ref. [43]. Extracted results from this study and those reported in Ref. [43] are shown in Fig. 15 for a crack with the constant aspect ratio of a/c=0.2 and different values of relative crack depth a/t.

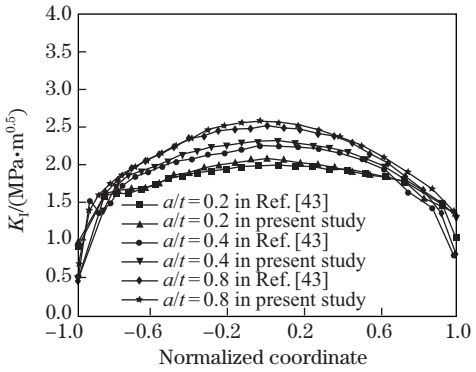

Fig. 15 Comparison of results between present study and Ref. [43]

As shown in Fig. 15, an appropriate compatibility can be found between the results, which confirms the presented approach in the modeling and analysis procedure.

7 Conclusions

In this paper, a comprehensive study of SIFs in rotating disks containing 3D semi-elliptical cracks under different working conditions is investigated. Based on this research, the following conclusions can be made:

(i) Propagation of cracks in the rotating disks initiates from the deepest point and free surfaces of crack front for the cracks with the aspect ratios of 0.4 to 0.6 and the aspect ratios of 0.8 to 1, respectively.

(ii) Regardless of mechanical properties of rotating disks, circumferential cracks are identified as crucial cracks in rotating disks.

(iii) The rotational velocity has more effects on SIFs of aluminum rotating disks than steel ones.

(iv) Patching reinforcement considerably decreases the SIF in the rotating disks. Employing thinner patches reduces the crack tip parameters considerably and can improve the fracture strength of the cracked specimens.

(v) Using a stiffer patch results in more reductions in the SIF. This implies that more considerable effects on the crack parameters take place when carbon/epoxy is used for composite patching instead of glass/epoxy.

(vi) Using the composite patch in the rotating disks has the maximum effect on radial cracks.

(vii) In the rotating disks regardless of mechanical properties of composite patches and orientation of cracks, the best value for a ply angle is known as 90°.

References

[1] Noda, N. A. and Xu, C. Controlling parameter of the stress intensity factors for a planar interfacial crack in three-dimensional bimaterials. *International Journal of Solids and Structures*, **45**, 1017–1031 (2008)

[2] Tweed, J., Das, S., and Rooke, D. The stress intensity factors of a radial crack in a finite elastic disc. *International Journal of Engineering Science*, **10**, 323–335 (1972)

[3] Tweed, J. and Rooke, D. The stress intensity factor of an edge crack in a finite elastic disc. *International Journal of Engineering Science*, **11**, 65–73 (1973)

[4] Ma, K. P. and Liu, C. T. Semi-weight function method on computation of stress intensity factors in dissimilar materials. *Applied Mathematics and Mechanics* (*English Edition*), **25**(11), 1241–1248 (2004) DOI 10.1007/BF02438279

[5] Jones, I. and Rothwell, G. Reference stress intensity factors with application to weight functions for internal circumferential cracks in cylinders. *Engineering Fracture Mechanics*, **68**, 435–454 (2001)

[6] Seifi, R. Stress intensity factors for internal surface cracks in autofrettaged functionally graded thick cylinders using weight function method. *Theoretical and Applied Fracture Mechanics*, **75**, 113–123 (2015)

[7] Chen, A. J. and Zeng, W. J. Weight function for stress intensity factors in rotating thick-walled cylinder. *Applied Mathematics and Mechanics* (*English Edition*), **27**(11), 29–35 (2006) DOI 10.1007/s10483-006-0105-1

[8] Wang, Y., Tham, L., Lee, P., and Tsui, Y. A boundary collocation method for cracked plates. *Computers and Structures*, **81**, 2621–2630 (2003)

[9] Fett, T. Stress intensity factors and T-stress for single and double-edge-cracked circular disks under mixed boundary conditions. *Engineering Fracture Mechanics*, **69**, 69–83 (2002)

[10] Kotousov, A., Berto, F., Lazzarin, P., and Pegorin, F. Three-dimensional finite element mixed fracture mode under anti-plane loading of a crack. *Theoretical and Applied Fracture Mechanics*, **62**, 26–33 (2012)

[11] Tsang, D., Oyadiji, S., and Leung, A. Two-dimensional fractal-like finite element method for thermoelastic crack analysis. *International Journal of Solids and Structures*, **44**, 7862–7876 (2007)

[12] Branco, R. and Antunes, F. Finite element modelling and analysis of crack shape evolution in mode-I fatigue middle cracked tension specimens. *Engineering Fracture Mechanics*, **75**, 3020–3037 (2008)

[13] Sanati, H., Amini, A., Reshadi, F., Soltani, N., Faraji, G., and Zalnezhad, E. The stress intensity factors (SIFs) of cracked half-plane specimen in contact with semi-circular object. *Theoretical and Applied Fracture Mechanics*, **75**, 104–112 (2015)

[14] Maschke, H. G. and Kuna, M. A review of boundary and finite element methods in fracture mechanics. *Theoretical and Applied Fracture Mechanics*, **4**, 181–189 (1985)

[15] Mavrothanasis, F. and Pavlou, D. Mode-I stress intensity factor derivation by a suitable Green's function. *Engineering Analysis with Boundary Elements*, **31**, 184–190 (2007)

[16] Belytschko, T. and Black, T. Elastic crack growth in finite elements with minimal remeshing. *International Journal for Numerical Methods in Engineering*, **45**, 601–620 (1999)

[17] Fett, T. and Bahr, H. Mode I stress intensity factors and weight functions for short plates under different boundary conditions. *Engineering Fracture Mechanics*, **62**, 593–606 (1999)

[18] Vigdergauz, S. An effective method for computing the elastic field in a finite cracked disk. *Engineering Fracture Mechanics*, **53**, 545–556 (1996)

[19] Rooke, D. and Tweed, J. The stress intensity factors of a radial crack in a finite rotating elastic disc. *International Journal of Engineering Science*, **10**, 709–714 (1972)

[20] Blauel, J., Beinert, J., and Wenk, M. Fracture-mechanics investigations of cracks in rotating disks. *Experimental Mechanics*, **17**, 106–112 (1977)

[21] Chan, S., Tuba, I., and Wilson, W. On the finite element method in linear fracture mechanics. *Engineering Fracture Mechanics*, **2**, 1–17 (1970)

[22] Gowhari-Anaraki, A., Djavanroodi, F., and Shadlou, S. Estimation of C^*-integral for radial cracks in annular discs under constant angular velocity and internal pressure. *American Journal of Applied Sciences*, **5**, 997–1004 (2008)

[23] Lorenzo, J. and Cartwright, D. Boundary element weight function analysis of a strip yield crack in a rotating disk. *Theoretical and Applied Fracture Mechanics*, **21**, 241–250 (1994)

[24] Xu, Y. L. Stress intensity factors of a radial crack in a rotating compound disk. *Engineering Fracture Mechanics*, **44**, 409–423 (1993)

[25] Bowie, O. L. and Neal, D. M. A modified mapping-collocation technique for accurate calculation of stress intensity factors. *International Journal of Fracture Mechanics*, **6**, 199–206 (1970)

[26] Isida, M. Arbitrary loading problems of doubly symmetric regions containing a central crack. *Engineering Fracture Mechanics*, **7**, 505–514 (1975)

[27] Pook, L. P., Berto, F., Campagnolo, A., and Lazzarin, P. Coupled fracture mode of a cracked disc under anti-plane loading. *Engineering Fracture Mechanics*, **128**, 22–36 (2014)

[28] Lin, X. and Smith, R. Fatigue growth prediction of internal surface cracks in pressure vessels. *Journal of Pressure Vessel Technology*, **120**, 17–23 (1998)

[29] Aliha, M., Bahmani, A., and Akhondi, S. Numerical analysis of a new mixed mode I/III fracture test specimen. *Engineering Fracture Mechanics*, **134**, 95–110 (2015)

[30] Knott, J. F. *Fundamentals of Fracture Mechanics*, Butterworths, London (1973)

[31] Hellen, T. On the method of virtual crack extensions. *International Journal for Numerical Methods in Engineering*, **9**, 187–207 (1975)

[32] Miyazaki, N., Ikeda, T., Soda, T., and Munakata, T. Stress intensity factor analysis of interface crack using boundary element method — application of contour-integral method. *Engineering Fracture Mechanics*, **45**, 599–610 (1993)

[33] Anderson, T. L. and Anderson, T. *Fracture Mechanics*: *Fundamentals and Applications*, CRC Press, Boca Raton (2005)

[34] Baker, A., Callinan, R., Davis, M., Jones, R., and Williams, J. Repair of Mirage III aircraft using the BFRP crack-patching technique. *Theoretical and Applied Fracture Mechanics*, **2**, 1–15 (1984)

[35] Baker, A. Repair of cracked or defective metallic aircraft components with advanced fibre composites — an overview of Australian work. *Composite Structures*, **2**, 153–181 (1984)

[36] Baker, A. Bonded composite repair of fatigue-cracked primary aircraft structure. *Composite Structures*, **47**, 431–443 (1999)

[37] Baker, A. *Crack Patching*: *Experimental Studies*, *Practical Applications*, *Bonded Repair of Aircraft Structures*, Springer, Berlin, 107–173 (1988)

[38] Rose, L. An application of the inclusion analogy for bonded reinforcements. *International Journal of Solids and Structures*, **17**, 827–838 (1981)

[39] Jones, R. and Callinan, R. Finite element analysis of patched cracks. *Journal of Structural Mechanics*, **7**, 107–130 (1979)

[40] Chung, K. H. and Yang, W. H. Fracture mechanics analysis on the bonded repair of a skin/stiffener with an inclined central crack. *Composite Structures*, **55**, 269–276 (2002)

[41] Bouiadjra, B. B., Belhouari, M., and Serier, B. Computation of the stress intensity factors for repaired cracks with bonded composite patch in mode I and mixed mode. *Composite Structures*, **56**, 401–406 (2002)

[42] Umamaheswar, T. V. and Singh, R. Modelling of a patch repair to a thin cracked sheet. *Engineering Fracture Mechanics*, **62**, 267–289 (1999)

[43] Nami, M. R. and Eskandari, H. Stress intensity factors in a rotating impeller containing semi-elliptical surface crack. *Mechanics Based Design of Structures and Machines*, **40**, 1–18 (2012)